Research on a Self-Coordinated Optimization Method for Distributed Energy Resources Targeting Risk Mitigation

Hongtao Li[1], Tian Hao[2], Zijin Li[1], Ergang Zhao[2,*], Chen Wang[1] and Lina Xu[2]

[1]*State Grid Beijing Electric Power Company Beijing, China*
[2]*Department of Electrical Engineering, Tsinghua University, Haidian District 100084, Beijing, China*
E-mail: zhaoeg10@163.com
[*]*Corresponding Author*

Received 26 March 2024; Accepted 13 May 2024

Abstract

This passage discusses a rapid restoration optimization strategy for short-term global coordination and the synergistic autonomous regulation of distributed energy sources based on a model predictive control framework. A short-term rapid recovery global coordination optimization model is established through the prediction of network states under abnormal conditions. This model includes the energy management of distributed energy sources and recovery plans for critical loads. In terms of the autonomous regulation of distributed energy sources, based on the results of global coordination optimization and aiming to minimize load shedding losses and grid losses, an ultra-short-term rolling control strategy is formulated using power output and

Distributed Generation & Alternative Energy Journal, Vol. 39_3, 659–690.
doi: 10.13052/dgaej2156-3306.39312

load switching as control variables. Finally, simulation analysis on the IEEE 33-node distribution network system indicates that the proposed model and method significantly accelerate the recovery speed of the distribution network and effectively enhance its resilience level.

Keywords: Rapid restoration, model predictive control, distribution network, distributed energy sources, resilience assessment.

1 Introduction

In the context of the construction of a new power system, a massive influx of heterogeneous distributed energy resources (DER), represented by energy storage, demand response, and distributed generation (DG), is gradually connecting to the distribution network and actively participating in its operation and control [1, 2]. The distribution network is evolving towards being actively powered, flexible, and characterized by high randomness [3, 4]. At the same time, the power grid faces increasingly complex internal and external threats, such as cascading faults, wide-frequency oscillations, network attacks, human errors, and extreme natural disasters [5]. When the transmission system is disrupted and unable to supply electricity to the distribution system in a timely manner, it can lead to widespread power outages [6], causing significant economic and social losses.

In response to the potential occurrence of major power outages, scholars both domestically and internationally have introduced the concept of a "resilient power grid" [7]. Its main features include actively coordinating internal and external resources of the power grid, proactively anticipating and defending against various disturbances, rapidly restoring critical loads, and achieving a high degree of self-healing [8, 9]. For the distribution network, it is possible to fully utilize the internal flexibility of various types of DERs to coordinate and formulate recovery plans. By quickly restoring critical loads before the transmission network recovers, the scope and losses of power outages can be minimized. Therefore, researching rapid emergency recovery strategies assisted by DERs for the distribution network, with a focus on enhancing its resilience from a self-healing perspective, is of great significance for energy security [10, 11].

Currently, various researches have been done to explore rapid recovery solutions for distribution networks assisted by a massive influx of heterogeneous DERs. This exploration mainly involves three aspects: distribution network partition, network restructuring, and load recovery. For the

optimization of distribution networks with a high proportion of DG, existing research mainly divides the network into multiple subsystems based on the performance of DG and the distribution of critical loads. Each subsystem is independently and parallelly recovered. Reference [12] proposes a novel optimal model for the islanding partition problem of active distribution networks (ADNs) considering the time series characteristics of the DGs and the loads, and the uncertainties of NDG outputs. Considering different operation modes of DGs, reference [13] presents a new reconfiguration formulation model in ADNs to investigate the flexibility of DGs in form isolated microgrids by changing their physical boundaries. To form more flexible islands for better load recovery, reference [14] proposes a dynamic island partition strategy based on the Dijkstra algorithm. It formulates a multi-objective multi-period optimization adjustment model considering controllable loads participating in dispatch However, the effectiveness of distribution network partition is influenced by the reconstruction of subsystem networks and load recovery results. Different partitioning schemes lead to differences in subsystem network structures and load recovery plans, subsequently affecting the overall system recovery efficiency. The three aspects are interdependent, mutually supportive, but many studies currently treat partition optimization in isolation, neglecting its interactive effects with subsequent recovery processes, which can lead to suboptimal results. Additionally, many studies have not considered the time-varying characteristics of the "source-load" relationship, relying solely on a single time cross-section as a reference for partition. This can result in power imbalances within subsystems during the distribution network recovery process.

In the optimization of subsystem network restructuring within distribution networks, existing research primarily focuses on establishing a secure and reliable network structure to ensure stable power supply, taking into account factors such as the start-up sequence of power sources, recovery paths, and the mutual influence between target network structures. Reference [15] proposes a novel optimisation method of network restructuring based on a two-layer unit-restarting framework for power system restoration. This two-layer framework includes network-layer and plant-layer unit restarting and the optimisation of the network restructuring is established as a multi-objective optimisation form. A loop-network reconfiguration optimization model is proposed in reference [16], in which a multi-scenario set of the wind power outputs including extreme scenarios is constructed since during the black-start restoration process the uncertainty of renewable energy outputs would aggravate the transmission line overloads. Although these studies

focus on the transmission network and microgrid levels, they can also provide valuable insights for network restructuring plans during the recovery process in distribution networks supported by a massive influx of flexible DERs. If the start-up sequence and recovery paths of power sources are planned in a coordinated manner and the interaction effects between the two aspects are comprehensively considered, better optimization results can be achieved for the rapid recovery of distribution networks with large scale of DERs.

Load recovery, as the ultimate goal of distribution network restoration, permeates the entire recovery process, with the final load recovery being influenced by the results of partition and network restructuring. Reference [17] presents a multi-objective optimization model to investigate the role of Battery Energy Storage Systems (BESSs) in power system restoration after blackouts. Based on flexible charging and discharging characteristics, leveraging BESSs can reduce circuit breaker operations and outage durations, thus accelerating the recovery speed of the power system after a blackout. Reference [18], considering the reliable power supply for the sensitive loads (e.g., industrial, commercial, and residential), proposes an analytical model for the restoration problem in distribution networks with self-healing features, optimizing actions like network reconfiguration, load rejection, and voltage regulation. A novel mathematical formulation that reduces binary variables is introduced, aiming for an efficient restoration plan with minimized de-energized nodes and self-healing actions. Reference [19] proposes a resilience enhancement model to optimize the preparatory operation of DGs against extreme weather events. The model minimizes the expected cost of energy not served and prioritize critical load restoration considering customer interruption costs, outage duration, and network constraints. However, few of the mentioned studies give sufficient consideration of the time-varying coupling characteristics of "source-load" across multiple time sections. Currently, the accuracy of intermittent DG and load power predictions still struggles to meet the demands of precise control, decreasing with increasing prediction duration. Model predictive control (MPC), as an advanced optimization algorithm, compensates for the shortcomings of prediction model accuracy through rolling optimization and feedback correction. It has shown significant effectiveness in suppressing disturbances and improving robustness, making it a research hotspot for dealing with uncertainty in large-scale integration of renewable energy sources [20]. Therefore, utilizing MPC for rapid recovery and precise control in ADNs becomes an effective technical means to address the aforementioned challenges.

In addressing the aforementioned issues, this study considers the time-varying characteristics of "source-load" within the distribution network and establishes a rapid emergency recovery strategy based on the MPC framework. The strategy combines short-term global coordination optimization and ultra-short-term subsystem autonomous regulation. Specifically, in the short-term global coordination optimization for emergency recovery, considering the mutually driving and supportive characteristics of subsystem recovery, a bi-level optimization model is constructed. The upper-level problem centers around the main power source as the regional core, with the goal of partitioning subsystems to satisfy the power supply radius. In the spatial domain, a preliminary partition model is established, utilizing a combination of the shortest path algorithm and breadth-first traversal methods to solve initial objectives and narrow down the scope of partition recovery strategy solutions. The lower-level model aims to minimize the total cost of emergency recovery and maximize the recovery of critical loads. In the temporal domain, a joint optimization model for partitioning and subsystem recovery is established to obtain the globally optimal recovery plan. Using the short-term global coordination optimization results as a baseline, the objective is to minimize load shedding losses and grid losses during the recovery process. This is achieved by optimizing the power output of sources and switching of loads to achieve the best power matching between DER and loads. This forms a rapid recovery strategy that combines subsystem rolling optimization with feedback correction. Finally, the effectiveness of the proposed method and model is validated using an improved IEEE 33-node distribution network system as an example.

The rest of this paper is organized as follows. The short-term global coordination optimization model for distribution network recovery is formulated in Section II. Section III introduces the ultra-short-term subsystem autonomous regulation model for distribution network recovery. And Section IV introduces the procedures of rolling optimization autonomous regulation and feedback correction optimization, and describes the solution method of the proposed model. Section V provides numerical results from case studies. Finally, this paper is concluded in Section VI.

2 Short-Term Optimization Model

The short-term global coordination optimization model for distribution network recovery is divided into two levels, including the preliminary partition

model at the upper level and the joint optimization model for partitioning and subsystem recovery at the lower level.

2.1 Upper Level

In this study, based on short-term predicted values of "source-load" at the moment of distribution network outage, preliminary partition is conducted in both spatial and temporal dimensions. The detailed steps are as follows:

(1) Determining the number of partitions. Analyze the time-varying characteristics of distributed resource output and determine the priority weights for the recovery of critical loads at the moment of the fault occurrence in the distribution network. Then choose energy storage with self-starting capability and good voltage and frequency regulation capabilities as the main power source for each subsystem. Based on the location of the main power source in each subsystem, determine the number of partitions required for the distribution network.

(2) Formulating the initial partition plan. Choose the reactance value (X) as the weight for the lines. Select the node where the black-start power source is located as the root node. Utilize Dijkstra's algorithm to calculate the shortest electrical distance (Q) from all load nodes to the root node. Set a preliminary partition threshold A_{Lim} and compare the shortest electrical distances from load nodes to different black-start power source nodes. Conduct preliminary partition on load nodes in the spatial dimension based on distances. For load nodes with distances less than the preliminary partition threshold, assign them to the respective partition. Nodes unable to be assigned to a partition due to distances smaller than the preliminary partition threshold are temporarily placed in the set of nodes Ψ_{net} to be partitioned further, awaiting additional optimization by the lower-level model.

(3) Correcting the initial partition targets based on the power supply radius. Use the main power source within each partition as the starting node, and define the power supply radius as the available output of the main power source at the outage moment. To account for the time-varying nature of "source-load," reserve a certain margin in the power supply radius. Utilize breadth-first traversal to search for first and second-level loads within the defined power supply radius. Determine the power source supply range by considering the available output of the main power source and check whether the power in the partition exceeds the limit to validate the rationality of the partition. If the power exceeds

the limit, prioritize load nodes with lower importance for recovery and assign them to the set of nodes to be partitioned further. If still not satisfied, modify the preliminary partition threshold A_{Lim} from Step 2) and redistribute the load. For other available DERs within the power supply range, aggregate their outputs and update the power supply radius and range accordingly. In case of overlapping power supply radii of main power sources, merge two partitions into one larger subsystem.

2.2 Lower Level

The preliminary partition results, based on the electrical parameters of the lines, exhibit a spatial characteristic with the subsystem's main power source at its core. However, for nodes that have not been partitioned, and where there is no significant difference in spatial distance to power sources, further consideration is required at the temporal level. All load nodes within the set of nodes to be partitioned further are considered decision variables. Utilizing a genetic algorithm, multiple partitioning schemes are randomly generated, forming a set of partitioning objectives (*S*). The objectives include minimizing the total emergency recovery cost and maximizing the resilience index. For each partitioning scheme in the objective set *S*, the subsystem recovery optimization model is invoked, ultimately solving for the optimal partitioning and optimal subsystem recovery scheme.

2.2.1 Partitioning model

2.2.1.1 *Objective*

The partitioning optimization model aims to minimize the total emergency recovery cost and maximize the resilience level. The recovery cost includes the time cost, line operation cost, and capacitor charging cost throughout the system recovery process. The following objective function is established:

$$\begin{cases} f_1 = \sum_{n=1}^{\Omega_{\mathrm{D}}} (T_n - \bar{T})^2 + \sum_{n=1}^{\Omega_{\mathrm{D}}} (g_{1,n} + g_{2,n} + T_n) \\ f_2 = R \end{cases} \tag{1}$$

$$\min F = \lambda_1 f_1 + \lambda_2 f_2 \tag{2}$$

where f_1 represents the total emergency recovery cost, composed of the recovery costs of all subsystems. Ω_{D} represents the total number of partitions. T_n represents the recovery time cost of subsystem *n*. $\bar{T}$ represents the average

recovery time cost of all subsystems and $\bar{T} = (\sum_{n=1}^{\Omega_{\mathrm{D}}} T_n)/\Omega_{\mathrm{D}}$. $g_{1,n}$ and $g_{2,n}$ represent the reactive power charging and switching number in the recovery path of subsystem *n*, respectively. $g_{1,n}$, $g_{2,n}$ and T_n together constitute the recovery cost of subsystem *n*. λ_1 and λ_2 are coefficients that influence the objective function and $\lambda_1 + \lambda_2 = 1$.

2.2.2 Constraints

2.2.2.1 *Power adequacy*

$$\sum_{i=1}^{\Omega_{\mathrm{G},d}} \beta_{\mathrm{G},n,i} P_{\mathrm{G},n,i} - \sum_{i=1}^{\Omega_{\mathrm{L},d}} \beta_{\mathrm{L},n,i} P_{\mathrm{L},n,i} > 0 \tag{3}$$

where $\Omega_{\mathrm{G},d}$ is the number of DERs in subsystem *n*. $\beta_{\mathrm{G},n,i}$ represents the start-up status of the *i*-th DER in subsystem *n*, where 1 indicates started and generating, and 0 indicates not started. $P_{\mathrm{G},n,i}$ is the active power output of the *i*-th DER in subsystem *n*. $\Omega_{\mathrm{L},d}$ is the number of load nodes in subsystem *n*. $\beta_{\mathrm{L},n,i}$ represents the recovery status of the *i*-th load node in subsystem *n*, where 1 indicates recovered, and 0 indicates unrecovered. $P_{\mathrm{L},n,i}$ is the active power of load *j* in subsystem *n*.

2.2.2.2 *DER output*

$$\begin{aligned} P_{\mathrm{G}m}^{\min} \le P_{\mathrm{G}m} \le P_{\mathrm{G}m}^{\max}, \quad m \in \Omega_{\mathrm{G}} \\ Q_{\mathrm{G}m}^{\min} \le Q_{\mathrm{G}m} \le Q_{\mathrm{G}m}^{\max}, \quad m \in \Omega_{\mathrm{G}} \end{aligned} \tag{4}$$

where $P_{\mathrm{G}m}$ is the active power output of the started DER. $Q_{\mathrm{G}m}$ is the reactive power output of the started DER. Ω_{G} is the set consisting of all DERs in the system.

2.2.2.3 *Node voltage*

$$U_i^{\min} \le U_i \le U_i^{\max}, \quad i \in \Omega_N \tag{5}$$

where U_i is the voltage magnitude at the already recovered node *i*. Ω_N is the set consisting of all already recovered nodes in the system.

2.2.2.4 *Node power balance*

$$\begin{cases} P_i = U_i \sum_{j=1}^{\Omega_{\mathrm{N}}} U_j (G_{ij} \cos\theta_{ij} + B_{ij} \sin\theta_{ij}) \\ Q_i = U_i \sum_{j=1}^{\Omega_{\mathrm{N}}} U_j (G_{ij} \cos\theta_{ij} + B_{ij} \sin\theta_{ij}) \end{cases} \tag{6}$$

where P_i and Q_i are the injected active and reactive power at node *i*. U_i and U_j are the voltage magnitudes at nodes *i* and *j*. G_{ij}, B_{ij} and θ_{ij} are the conductance, susceptance, and voltage phase angle difference between nodes *i* and *j*, respectively.

2.2.2.5 *Transmission line capacity limit*

$$|P_{\mathrm{L}l}| \leq P_{\mathrm{L}l}^{max}, l \in \Omega_{\mathrm{L}} \tag{7}$$

where $P_{\mathrm{L}l}$ represents the active power transmitted in line *l*.

2.2.2.6 *Radiation operation*

$$H \in \Omega_{\mathrm{H}} \tag{8}$$

where Ω_{H} represents the set of radiation topology structures in the distribution network.

2.2.3 Subsystem recovery model

The subsystem recovery model is to reconstruct the de-energized network, jointly optimize the load recovery sequence and charging paths, obtain the target network to be restored, and ultimately achieve the continuous and reliable power supply to the internal important loads. This paper proposes an elastic operation strategy based on MPC to achieve real-time optimization and adjustment of the power output and load switching quantities.

2.2.3.1 *Objective*

For each subsystem, the following objective functions are established:

$$\max G = \frac{\sum_{i=1}^{\Omega_{\mathrm{L},n}} \int_{t_{r,i}}^{t_{r,i+T_0}} \beta_{L,n,i}(t)\rho_{L,n,i}(t)P_{L,n,i}(t)dt}{\sum_{l=1}^{\Omega_{l,n}} Z_l}\Omega_{\mathrm{L},n} \tag{9}$$

where $\Omega_{\mathrm{L},n}$ is the number of all load nodes in subsystem *n*. $\Omega_{l,n}$ is the number of all lines in subsystem *n*. $t_{r,i}$ represents the time at which load node *i* in subsystem *d* is supplied during recovery. $t_{r,i+T_0}$ represents the time at which the system fault is resolved, and normal operation is restored in subsystem *n*. $\beta_{L,d,i}$ represents recovery status of load node *i* in subsystem *n* (1 for recovered, 0 for not recovered). $\rho_{L,n,i}(t)$ represents priority weight for load node *i* in subsystem *n* at time *t*. $P_{L,n,i}(t)$ represents active power of load node *i* in subsystem *n* at time *t*. Z_l represents the weight of line *l*. The constraints for the subsystem recovery model are similar to Equations (3) to (8).

2.2.3.2 *Line importance assessment indices*

This paper considers both efficiency and risk when establishing the skeleton network, taking into account the impact of line operation time, charging capacitance, and switch operations on line weights. Line weights are set to evaluate the importance of lines, and optimization results in the recovery path composed of high-importance lines.

2.2.3.3 *Weight assignment for line operation time*

The evaluation criterion for the operation time of each line in the emergency recovery process of the distribution network is defined as the time operation weight *t*. This weight measures the time consumed by a line from the start of charging to the completion of charging. In practical systems, the operation time for each line is typically divided into optimistic estimate time *A*, pessimistic estimate time *B*, and most likely estimate time *M* based on the experience of operators. The actual required time for the recovery of each line, denoted as t_l, follows a Beta distribution between *A* and *B* [21]. For the operation time of a specific line l, its expected value $E(t_l)$ and variance σ_l are given by:

$$E(t_l) = \frac{A + 4M + B}{6} \tag{10}$$

$$\sigma_l = \left(\frac{B - A}{6}\right)^2 \tag{11}$$

where $l \in \psi_{\mathrm{L}}$ and ψ_{L} represents the set of all lines in the system. Assuming there are L lines forming the power delivery path located at a specific node *i*, the mean and variance of the operation time for this recovery path are given by:

$$T_i = \sum_{l=1}^{L} E(t_l) \tag{12}$$

$$\sigma_i = \sqrt{\sum_{l=1}^{L} \sigma_l^2} \tag{13}$$

2.2.3.4 *Cost weight for line recovery*

The total charging capacitance is crucial to consider during network restructuring as excessive capacitance can impact system safety, leading to overvoltage conditions on the lines, especially under no-load or light-load conditions.

Managing and optimizing this capacitance is essential for ensuring the reliability and safety of the reconfigured distribution network. The total charging capacitance on the recovery path for load node *i* can be expressed as:

$$C_L = \sum_{l \in \Omega_{\mathrm{L}}} C_l \tag{14}$$

where C_L represents the total charging capacitance, and C_l is the charging capacitance with line *l*.

If we consider the recovery cost weight W_l for line *l* as an indicator of the difficulty level in the recovery process, setting the recovery cost weight based solely on the impact of line charging capacitance may lead to the formation of multiple recovery paths composed of lines with small charging capacitance, replacing the recovery of a single line. This, in turn, can result in frequent switch operations on the lines. To address this, the recovery cost weight for line *l* can be set as:

$$W_l = C_l + S_l \tag{15}$$

where S_l represents the operating cost of closing and opening the switch for line *l*. Typically, circuit breakers are installed at both ends of the line, and during recovery, closing the breaker is necessary. Assuming the operating cost for each line S_l is the same, adjusting the value of S_l allows for tuning the influence of both line charging capacitance and switch operation frequency on the optimization of the recovery path.

2.2.3.5 *Weight of each line*

The weight of a line Z_l is determined by considering two evaluation indicators: the recovery cost weight W_l and the time operation weight t_l. The weight of a line is set as:

$$Z_l = \mu_1 W_l + \mu_2 t_l \tag{16}$$

where μ_1 and μ_2 are parameters that adjust the balance between time operation and recovery cost, and $\mu_1 + \mu_2 = 1$. When the time operation weight and the recovery cost weight of a line are smaller, the overall weight of the line will be smaller.

3 Ultra-Short-Term Model

The deviations in the forecasted power of the "source-load" can lead to power imbalances and increased network losses, thereby raising the risk of failure in

distribution network recovery. To address this issue, a self-regulating control strategy is proposed within the ultra-short-term subsystem. This strategy uses the short-term global coordinated optimization scheme as a baseline and relies on real-time updates of wind speed, solar irradiation, and load ultra-short-term forecast information. The approach involves employing a rolling optimization method to construct the optimal control sequence within a given time interval $(\tau + \Delta t)$ at the τ-th moment. This real-time rolling optimization is designed to determine the optimal adjustments to DERs output and load shedding increments. By incorporating real-time data on energy generation and demand fluctuations into the self-regulating control strategy, the system can make more accurate predictions and adjustments, leading to improved coordination and optimization of energy sources to meet demand and enhance the recovery strategy's effectiveness. The primary objectives are to ensure power balance within each subsystem, enhance operational stability, and improve power quality. The rolling control time domain is defined as T_{c}, with a sampling time interval denoted as Δt, and the optimization goals include minimizing load shedding losses and network losses.

The objective function for the self-regulating control of the subsystem within the ultra-short-term domain is designed to minimize outage losses by controlling the amount of load shedding or restoration based on the load recovery situation obtained from the short-term global coordinated optimization scheme. The goal is to achieve the optimal power matching between the "source-load" in the distribution network. The objective y_1 is formulated as:

$$y_1 = \min \sum_{t=\tau}^{\tau+T_2} \left[\sum_{i=1}^{\Omega_{\mathrm{L},n}} (1 - \beta_{\mathrm{L},n,i}(\tau)) \rho_{\mathrm{L},n,i}(\tau) (P_{\mathrm{L},n,i}(\tau) + \Delta P_{\mathrm{L},n,i}(\tau)) \right] \tag{17}$$

where $P_{\mathrm{L},n,i}(\tau)$ represents the actual measured load power at node *i* in subsystem *n* at time τ. $\Delta P_{\mathrm{L},n,i}(\tau)$ represents the short-term forecasted change in load power at node *i* in subsystem *n* at time τ.

Further, using the load recovery state obtained from the optimization of y_1 as a reference and based on short-term forecasted information of wind speed, solar irradiation, and load, the objective of subsystem autonomous control is to minimize network loss within the controlled subsystem by adjusting the controllable DER output power to reduce "source-load" power imbalance.

The subsystem autonomous control objective function y_2 is expressed as:

$$y_2 = \min \sum_{t=\tau}^{\tau+T_2} [\Delta P_{\text{loss},n}(\tau)] \tag{18}$$

where $\Delta P_{\text{loss},n}(\tau)$ represents the network loss in subsystem *n* at time τ.

The power balance, DER output, node voltage constraints, etc., have been described earlier, i.e., constraints (4)–(6).

Energy storage has a fast start-up capability, and its state of charge (SOC) remains relatively constant [22]. It can provide stable voltage and frequency support for other power sources during the recovery process. Considering energy storage charging and discharging power constraints and energy storage state of charge constraints [23], they are expressed as follows.

$$-P_{\text{ES,N}} \le P_{\text{ES}}(t) \le P_{\text{ES,N}} \tag{19}$$

$$S_{\text{SOC,ES,min}} \le S_{\text{SOC,ES}}(t) \le S_{\text{SOC,ES,max}} \tag{20}$$

where $P_{\text{ES,N}}$ is the rated power of the energy storage. $S_{\text{SOC,ES,min}}$, $S_{\text{SOC,ES,max}}$ and $S_{\text{SOC,ES}}(t)$ are the lower and upper limits of the state of charge of the energy storage and the state of charge during the recovery process, respectively.$S_{\text{SOC,ES}}(t)$ can be calculated as:

$$S_{\text{SOC,ES}}(t) = 1 - \delta) + \left(\eta_{\text{c}} P_{\text{ES}}^{\text{c}}(t) - \frac{P_{\text{ES}}^{\text{d}}(t)}{\eta_{\text{d}}}\right) \Delta t / S_{\text{s}} \tag{21}$$

where δ is the self-discharge rate of the energy storage. η_{c} and η_{d} are the charging and discharging efficiencies, respectively. $P_{\text{ES}}^{\text{c}}(t)$ and $P_{\text{ES}}^{\text{d}}(t)$ are the charging and discharging powers at time *t*, respectively. S_{s} is the capacity of the energy storage.

4 Solving Methods

To reduce load shedding losses and network losses during the recovery process and achieve the optimal matching between different types of DERs and loads, the following subsystem rolling optimization and feedback correction control strategy is proposed. It is assumed that the distribution network is divided into subsystems A and B.

4.1 Rolling Autonomous Control Strategy in the Real-time Stage

Step 1: Based on the current time *k* and the measured "source-load" state $x(\tau)$ within the subsystem, obtain short-term predictions of active power output for wind and solar power, as well as the power consumption of each node, using the prediction model. Further deduce the operating state of the subsystem and calculate the power deviation between DERs and loads. Determine whether load shedding is needed in the future time $\tau+1, \tau+2, \ldots, \tau+T_{\mathrm{c}}$. If no load shedding is required, proceed directly to step 3; otherwise, proceed to step 2.

Step 2: If load shedding is needed, optimize the load shedding amount for the future time $\tau+1, \tau+2, \ldots, \tau+T_{\mathrm{c}}$ based on the objective function y_1. Use the first optimal solution from the control sequence to minimize load shedding losses. Compare the expected load shedding losses. If subsystems A and B all have positive or negative power deviations, perform rolling optimization and autonomous control to match DERs with loads until load shedding losses are reduced to a reasonable level. Proceed to step 3. If subsystem A, after optimization, requires cutting off a portion of the load due to negative power deviation, resulting in load shedding losses significantly exceeding expectations, and subsystem B still have large positive deviations after recovering important loads, it indicates that the partitioning scheme in the short-term global coordination optimization of the distribution network recovery needs feedback adjustment. Proceed to global feedback correction.

Step 3: With the optimized load recovery status as a reference, use the objective function y_2 to further optimize the power output of the power sources. Achieve the best matching between DERs and loads. Update the subsystem state to $x(\tau+1)$ at time $\tau+1$, and repeat the above operation steps.

4.2 Feedback Correction Control Strategy

The time-varying characteristics of "source-load" and the preliminary partition limit can affect subsystem recovery. It is necessary to adjust the partitioning scheme based on the rolling optimization of the subsystem.

Step 1: Based on the preliminary partition scheme, reassign the loads in the set of nodes awaiting partitioning. According to the power deviation between DERs and loads obtained from rolling optimization and control, and with reference to the priority recovery weight $\rho_i(t)$ reassign the loads originally allocated to subsystem A to prioritize subsystem B. If after the reallocation,

the power deviations in subsystems A and B are all within a reasonable range, then end the process. Otherwise, proceed to step 2.

Step 2: Reduce the preliminary partition limit, expand the set of nodes awaiting partitioning, and re-execute step 1. If there are still subsystems with power deviations, proceed directly to step 2 of the real-time rolling autonomous control strategy. If load shedding is required to remove excessive loads, then end the global feedback correction.

4.3 Model Solving

This article employs a combination of genetic algorithm and Floyd algorithm to solve the partitioning and subsystem recovery optimization model. The load node variables in the set of partition nodes are encoded as real integers, while the load node variables in each subsystem use permutation encoding. For each partitioning scheme's subsystem, load recovery nodes and sequences are randomly generated. The Floyd algorithm is then invoked to search for recovery paths for each sequence. This process yields the global optimal solution for partitioning and subsystem recovery in the entire system.

5 Case Study

In this section, an improved IEEE 33-node distribution network system is employed for simulation analysis, as depicted in Figure 1. The system comprises a total of 37 branches, with dashed lines representing 5 tie-switch branches. Details of all line parameters, node load levels, types, and load demand can be found in the appendix.

The time from fault outage to recovery is assumed to be 2 hours, and transient quantities such as excitation surge currents generated by starting substations and impact currents generated by asynchronous motors

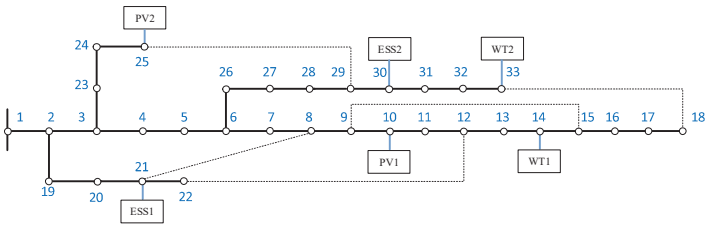

Figure 1 Improved IEEE 33 node distribution network system.

during emergency recovery are not considered. It is assumed that DERs are connected to nodes 10, 14, 21, 25, 30, and 33. The energy storage system has an SOC of 80% at the time of outage and can provide sustained power discharge with a maximum power of 2 hours. The detailed parameters of DERs and typical daily renewable energy outputs and load demand curves can be also found in the appendix.

5.1 Short-term Optimization Results

Assuming that at 14:00, a fault occurs in the transmission network system, leading to a widespread power outage in the IEEE 33-node distribution network. At this time, the available generation capacity of photovoltaic and wind power is approximately 64% and 62%, respectively, with a total available output of 2714kW.

5.1.1 Results of preliminary partitioning

Based on the characteristics of DER output and considering its available output, start-up time, load capability, as well as voltage and frequency regulation capabilities, nodes 21 and 30 with energy storage are chosen as the main power sources for subsystems. Considering the locations of ESS1 and ESS2, the number of partitions is determined to be 2, dividing the distribution network into subsystem A and subsystem B, each supported by energy storage as the main power source for parallel recovery of voltage and frequency. This study sets the initial partition limit $A_{\text{lim}} = 1$. Taking nodes 21 and 30 as root nodes and using the line electrical parameters as weights, the Dijkstra algorithm is invoked to perform the initial partitioning of the system nodes, resulting in the set of nodes to be partitioned $\Psi_{\text{net}} = \{$node 3, node 4, node 5, node 6, node 15, node 23, node 26$\}$. The preliminary partitioning results are shown in Figure 2.

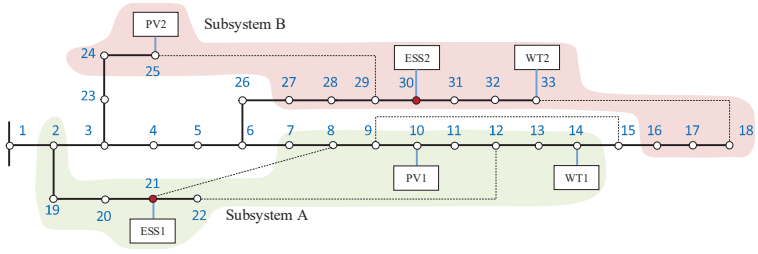

Figure 2 Preliminary partition results.

It can be seen that the initial partitioning only considers the line electrical parameters and does not account for the "source-load" matching within subsystems. Further adjustments to the partition are made based on the power supply radius. Based on the "source-load" status at the time of the outage, the initial partition is corrected according to the power supply radius. Using nodes 21 and 30 as the main power supply points for subsystems A and B, the initial power supply radii for subsystems A and B are set to 500 and 800 kW, respectively, with a 20% reserve capacity. Breadth-first traversal is used to prioritize the search for primary and secondary loads, determining the power supply range of the main power sources. After confirming that the important load power in subsystems A and B does not exceed the limit, the rationality of the partition is verified.

5.1.2 Results of partitioning and subsystem recovery

Since the initial partition is based on line electrical parameters and is centered around the main power sources in the spatial dimension, for undivided nodes with no significant differences in spatial distance to the two main power sources, further division is required on the temporal dimension. Using the load nodes in the set of nodes to be partitioned as control variables for partition optimization and the load nodes in subsystems A and B as control variables for grid reconstruction and load recovery optimization, the emergency recovery plan for the distribution network is further optimized through joint partitioning and subsystem recovery. The partition results, load recovery sequence, and charging path results are shown in Figure 3, where yellow solid circles represent loads that have been restored at these nodes, hollow circles represent loads that have not been restored, orange thick solid lines represent charged lines that have been opened and closed, and dashed lines represent lines that are disconnected.

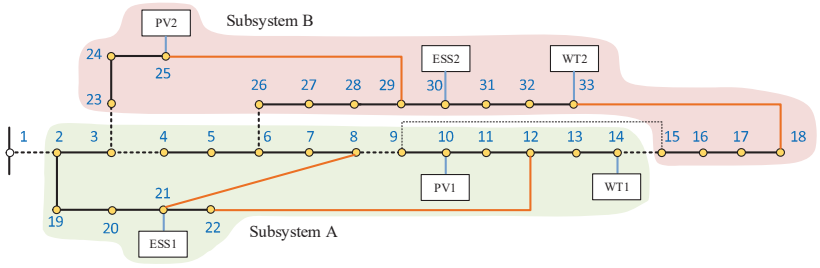

Figure 3 Global coordination and optimization results before black start.

The set of nodes to be partitioned includes load nodes 3, 4, 5, and 6, which are allocated to subsystem A, and load nodes 15, 23, and 26, which are allocated to subsystem B. The specific steps for solving the recovery plan within each subsystem are described in detail as follows:

In subsystem A: The energy storage ESS1 at node 21 is self-started as the main power source using V/F control. Stable voltage and frequency are established. Connection is established with the photovoltaic DER1 at node 10 and the wind WT1 at node 14. PV1 and WT1 operate as secondary power sources using PQ control. Priority is given to sequentially restore the first-level loads at nodes 8, 21, 9, and 3, ensuring their safe and stable power supply. Next, the second-level loads at nodes 2, 12, 19, 13, and 6 are sequentially restored, meeting their power supply needs on the basis of uninterrupted power supply to the first-level loads. Finally, considering the remaining available output within subsystem A, the third-level loads at nodes 7, 20, 10, 14, 22, 11, 5, and 4 are sequentially restored. The calculated time for the entire subsystem A to recover from the outage is 18 minutes.

In subsystem B: The energy storage ESS2 at node 30 is self-started as the main power source using V/F control. Stable voltage and frequency are established. Connection is established with the photovoltaic PV2 at node 25 and the wind WT2 at node 33. PV2 and WT2 operate as secondary power sources using PQ control. Priority is given to sequentially restore the first-level loads at nodes 24, 32, and 29, ensuring their safe and stable power supply. Next, the second-level loads at nodes 25, 23, 28, and 16 are sequentially restored, meeting their power supply needs on the basis of uninterrupted power supply to the first-level loads. Finally, considering the remaining available output within subsystem B, the third-level loads at nodes 33, 30, 18, 31, 17, 15, 27, and 26 are sequentially restored. The calculated time for the entire subsystem B to recover from the outage is 18 minutes.

5.2 Results of Ultra-Short Term Subsystem Autonomous Control

After completing grid reconstruction and load restoration in both subsystems A and B, the rolling optimization autonomous control and feedback correction operations are conducted starting from 14:20. Based on the current measured "source-load" status and the short-term global coordination optimization results, the real-time rolling optimization autonomous control and feedback correction are performed according to the ultra-short-term forecast values of wind and photovoltaic active power outputs and load power at

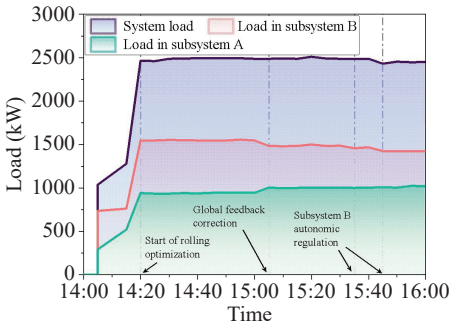

Figure 4 Load recovery in distribution network system.

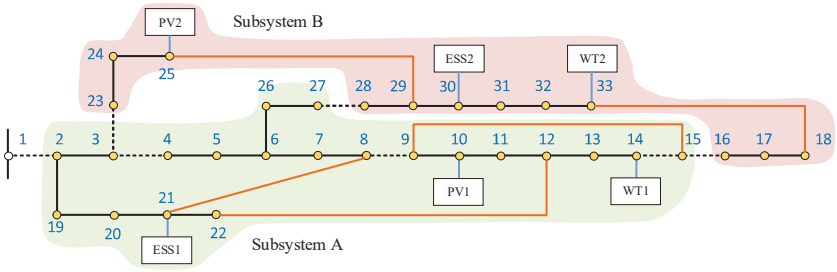

Figure 5 Diagram after global feedback correction at time 15:05.

each node (see Appendix Figure A1). The load recovery situation in the distribution network system is shown in Figure 4.

According to the results analysis, the power outage occurred at 14:00 when wind and solar resources are abundant enough to support the recovery of all loads in the system. As the sunlight gradually decreased in the afternoon, photovoltaic output reduces. Through rolling optimization and feedback correction to adjust the generator output, and cutting off some low-priority recovered loads, the system remains safe and stable.

At 15:05, during rolling optimization, there is a power mismatch between DERs and loads in subsystem B, leading to a negative deviation. Through optimization, it is found that subsystem B needed to cut off some low-priority recovered loads to maintain power balance. However, at this time, subsystem A still has a positive deviation in power, indicating that the partitioning scheme in the short-term global coordination optimization needed feedback correction. Therefore, a global feedback correction operation is executed, as shown in Figure 5.

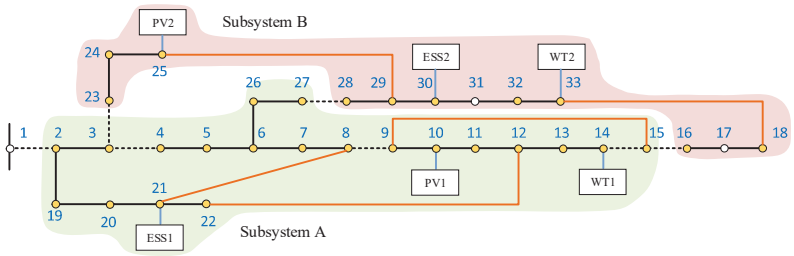

Figure 6 Diagram after self-regulation of subsystem B at time 15:45.

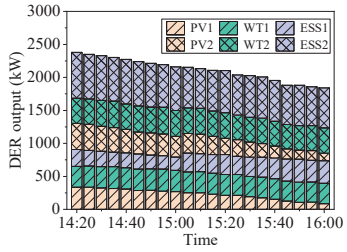

Figure 7 Power output diagram in the system.

When rolling optimization reaches 15:35, as the sunlight intensity decreases, the available output of photovoltaics gradually decreases, and the demand for residential load increases, leading to a negative deviation in subsystem B. This deviation cannot satisfy the power balance constraint within subsystem B. Since the positive deviation in subsystem A is relatively small, the global feedback correction is not triggered. It is necessary to autonomously control and finally cut off the load node 17 to achieve balance. Continuing the rolling optimization until 15:45, as the sunlight intensity further decreases, a negative deviation occurs in subsystem B. To address this, it is necessary to autonomously control and cut off the load node 31 with lower priority recovery weight. The result after autonomous control is shown in Figure 6.

Based on the short-term forecast information of wind speed, solar irradiation, and load, by controlling the controllable DER output, the power difference between "source and load" is reduced, aiming to minimize network losses within the control domain of the subsystem. The output situations of each DER are depicted in Figure 7. Utilizing energy storage helps smooth the fluctuations in wind and solar output and load demand, building upon the effective utilization of renewable energy resources for power generation.

Table 1 Calculation efficiency of different models

Model		Solution Time/s	#Iter
Short-term global coordinated optimization model	Preliminary partition model	6.447	–
	Joint optimization model of partition and subsystem recovery	3210.214	19
Ultra-short-term subsystem self-regulation model	Load switching variation and subsystem network loss optimization	4.256	–

5.3 Computational Performances

To further verify the applicability of the proposed model framework for ultra-short-term rolling control, an analysis of the model calculation efficiency is conducted, and the results are shown in Table 1. According to the results in Table 1, for the short-term global coordination optimization model, its preliminary partitioning model exhibits high calculation efficiency. After solving the preliminary partition, only a small number of nodes remain to be partitioned, significantly reducing the scope of partition recovery strategy and decreasing the computation load of the joint optimization model for partitioning and subsystem recovery. For the ultra-short-term subsystem autonomous control model, its calculation is mainly fine-tuning based on short-term optimization. The actual model computation time can be controlled within 10 seconds. Therefore, the model's calculation efficiency meets the requirements of ultra-short-term rolling control.

5.4 Comparative Analysis of Various Recovery Schemes

Taking the method proposed in this paper as Method 1 (M1), single-time-section optimization as Method 2 (M2), and multiple-time-section open-loop optimization as Method 3 (M3), a comparative analysis of the effects of these three methods on emergency recovery schemes in distribution networks is conducted, and the results are presented in Table 2.

It can be observed that the proposed method M1, which combines MPC for short-term global coordination optimization and ultra-short-term subsystem autonomous control, achieves a higher total recovered load, the least blackout load, and a relatively higher resilience assessment indicator. M2, which considers only a single-time section, results in a failure of system recovery due to power imbalance affecting normal load supply when the blackout continues until 15:05. Moreover, it has the minimum total recovered

Table 2 Comparison of recovery schemes

Duration of Power Outage	Methods	Total Restored Load/(kWh)	Number of Power Loss Loads	Resilience Index (R)
	M1	4045.417	2	66.287
14:00-16:00	M2	1993.296	32	0.0160
	M3	4129.939	4	13.563

load and the lowest resilience assessment indicator. M3, considering the coupling of multiple time sections, shows a noticeable improvement in the overall effect of the recovery scheme compared to M2. However, it neglects the mutual influence between sections and lacks feedback correction, leading to a direct cut-off of part of the load when the blackout continues until 15:05, revealing significant deficiencies in the recovery scheme.

6 Conclusion

This paper is aimed at the situation where a large-scale blackout occurs in the distribution network due to a fault in the transmission network. The new demand arises for utilizing abundant distributed energy resources (DERs) to assist in the rapid self-healing of critical loads in the distribution network. The paper takes into full consideration the time-varying characteristics of "source-load" and their impact on the system recovery process. Based on the model predictive control (MPC) framework, a rapid emergency recovery strategy for distribution networks is constructed, combining short-term global coordination optimization and ultra-short-term subsystem autonomous control. By progressively refining the predictive information and rolling optimization with feedback correction within subsystem recovery processes, the paper ensures the safe operation of the system.

Case studies show that compared to single-time-section optimization and open-loop optimization without feedback correction, the proposed method has significant advantages in ensuring power supply to critical loads, reducing recovery costs, and improving system resilience. Additionally, energy storage, as a critical supporting power source in the distribution network recovery process, is significantly influenced by the uncertainty of available capacity at the time of the blackout. Similarly, the duration of distribution network recovery will also inversely affect the utilization of energy storage resources and the formulation of recovery plans. In future, by diversifying storage technologies, optimizing energy storage configurations, and implementing flexible control strategies, robust recovery plans can be developed to address

uncertain energy storage availability during blackouts. Optimization configurations for energy storage devices will be developed based on factors such as the penetration rate of wind/solar power and resource availability within regional distribution networks. Coordinated control strategies for wind and solar power will be formulated to meet the demands of reliability, stability, and continuity in power supply, collectively supporting the rapid emergency recovery of distribution networks under the integration of abundant distributed resources.

Appendix

Table A1 Node parameters of IEEE 33 distribution network

Bus No.	Bus Type	Load Type	Load Importance Rating	Active Power/kW	Reactive Power/kVar
1	3	–	–	–	–
2	1	Commercial	2	90	50
3	1	Government	1	80	30
4	1	Resident	3	110	70
5	1	Commercial	3	50	20
6	1	Resident	2	50	10
7	1	Commercial	3	190	90
8	1	Government	1	190	90
9	1	Medical	1	50	10
10	1	Commercial	3	50	10
11	1	Resident	3	35	20
12	1	Commercial	2	50	25
13	1	Resident	2	50	25
14	1	Resident	3	110	70
15	1	Resident	3	50	0
16	1	Commercial	2	50	10
17	1	Resident	3	50	10
18	1	Commercial	3	80	30
19	1	Resident	2	80	30
20	1	Commercial	3	80	30
21	1	Medical	1	80	30
22	1	Resident	3	80	30
23	1	Commercial	2	80	40

(*Continued*)

Table A1 Continued

Bus No.	Bus Type	Load Type	Load Importance Rating	Active Power/kW	Reactive Power/kVar
24	1	Government	1	410	190
25	1	Commercial	2	410	190
26	1	Resident	3	50	15
27	1	Resident	3	50	15
28	1	Resident	2	50	10
29	1	Medical	1	110	60
30	1	Commercial	3	190	590
31	1	Resident	3	140	60
32	1	Medical	1	200	90
33	1	Resident	3	50	30

Note: In the column of load importance rating, "1" means the first-level load, i.e., the most important load.

Table A2 Branch parameters of the IEEE 33 node distribution network

Branch No.	From Bus	To Bus	Resistance	Reactance	Operation Time
1	1	2	0.09	0.05	2
2	2	3	0.49	0.25	1
3	3	4	0.37	0.19	2
4	4	5	0.38	0.19	1
5	5	6	0.82	0.71	1
6	6	7	0.19	0.62	1
7	7	8	0.71	0.24	1
8	8	9	1.03	0.74	2
9	9	10	1.04	0.74	1
10	10	11	0.20	0.07	1
11	11	12	0.37	0.12	2
12	12	13	1.47	1.16	1
13	13	14	0.54	0.71	1
14	14	15	0.59	0.53	2
15	15	16	0.75	0.55	1
16	16	17	1.29	1.72	1
17	17	18	0.73	0.57	2
18	2	19	0.16	0.16	1
19	19	20	1.50	1.36	2
20	20	21	0.41	0.48	2
21	21	22	0.71	0.94	1
22	3	23	0.45	0.31	1

(*Continued*)

Table A2 Continued

Branch No.	From Bus	To Bus	Resistance	Reactance	Operation Time
23	23	24	0.90	0.71	1
24	24	25	0.90	0.70	1
25	6	26	0.20	0.10	2
26	26	27	0.28	0.14	1
27	27	28	1.06	0.93	1
28	28	29	0.80	0.70	1
29	29	30	0.51	0.26	2
30	30	31	0.97	0.96	2
31	31	32	0.31	0.36	1
32	32	33	0.34	0.53	2
33	21	8	2	2	1
34	9	15	2	2	1
35	12	22	2	2	1
36	18	33	0.5	0.5	2
37	25	29	0.5	0.5	1

Table A3 DER parameters in distribution network

Bus No.	Generation Type	Rated Active Power/kW	Start-up Time/min	Ramping-up Rate/ (%/min)	Voltage and Frequency Regulation Ability	Self-start Ability
10	PV1	600	2	5.5	Weak	×
14	WT1	500	2	5	Weak	×
21	ESS1	500	1	6	Strong	v
25	PV2	700	2	5	Weak	×
30	ESS2	700	1	5.5	Strong	v
33	WT2	600	2	4.5	Weak	×

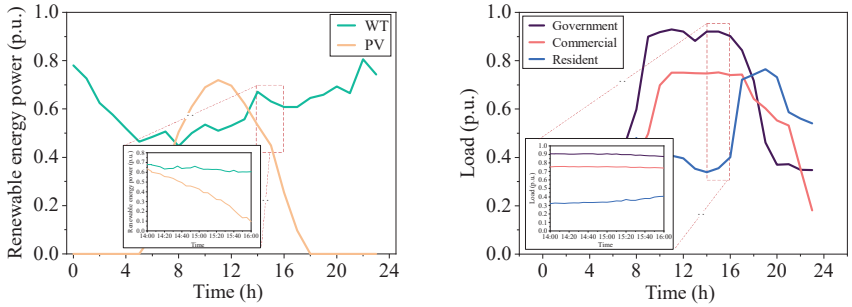

(a) Renewable energy typical daily output curve (b) Typical demand curve of various loads

Figure A1 Renewable energy output and load demand in a typical day.

Funding Statement

This research was supported by the project "Key Technology and Demonstration of Urban-Suburban New Distribution Network Collaborative Planning and Operation Based on Hierarchical Autonomy and Regional Mutual Aid" (Project No.: 5400-202211 507A-3-0-SF).

References

[1] S. Mirsaeidi, X. Dong, S. Shi, and D. Tzelepis, "Challenges, advances and future directions in protection of hybrid AC/DC microgrids," IET Renewable Power Generation, vol. 11, no. 12, pp. 1495–1502, Oct. 2017.

[2] B. Shen et al., "Research on the Morphological Development of New Distribution Networks," in 2022 Asia Power and Electrical Technology Conference (APET), Nov. 2022, pp. 143–149.

[3] S. Mallapaty, "How China could be carbon neutral by mid-century," Nature, vol. 586, no. 7830, pp. 482–483, Oct. 2020.

[4] D. Wu, J. Su, Z. Chen, and H. Liu, "Effects of Distributed Generation on Carbon Emission Reduction of Distribution Network," Distributed Generation & Alternative Energy Journal, pp. 57–82, 2024.

[5] L. Xu, Q. Guo, Y. Sheng, S. M. Muyeen, and H. Sun, "On the resilience of modern power systems: A comprehensive review from the cyber-physical perspective," Renewable and Sustainable Energy Reviews, vol. 152, p. 111642, Dec. 2021.

[6] D. K. Mishra, M. J. Ghadi, A. Azizivahed, L. Li, and J. Zhang, "A review on resilience studies in active distribution systems," Renewable and Sustainable Energy Reviews, vol. 135, p. 110201, Jan. 2021.

[7] S. A. Modaberi, S. Tohidi, S. G. Zadeh, and T. G. Bolandi, "A review of power system resilience assessment and enhancement approaches by focusing on wind farms and wind turbines," IET Renewable Power Generation, vol. 17, no. 9, pp. 2391–2410, 2023.

[8] C.-C. Liu, "Distribution Systems: Reliable But Not Resilient? [In My View]," IEEE Power and Energy Magazine, vol. 13, no. 3, pp. 93–96, May 2015.

[9] D. Chippada and M. D. Reddy, "Optimal Placement and Sizing of Renewable and Non-Renewable Resources in Smart Grid," Distributed Generation & Alternative Energy Journal, pp. 1033–1054, Mar. 2023.

[10] S. Ghasemi and J. Moshtagh, "Distribution system restoration after extreme events considering distributed generators and static energy storage systems with mobile energy storage systems dispatch in transportation systems," Applied Energy, vol. 310, p. 118507, Mar. 2022.

[11] F. Fayaz and G. L. Pahuja, "Optimal Control of Hybrid Power System Integrated with Distributed Generation and Electric Vehicle," Distributed Generation & Alternative Energy Journal, pp. 189–214, 2023.

[12] J. Zhao et al., "An islanding partition method of active distribution networks based on chance-constrained programming," Applied Energy, vol. 242, pp. 78–91, May 2019.

[13] T. Zhao, B. Chen, S. Zhao, J. Wang, and X. Lu, "A Flexible Operation of Distributed Generation in Distribution Networks With Dynamic Boundaries," IEEE Transactions on Power Systems, vol. 35, no. 5, pp. 4127–4130, Sep. 2020.

[14] Z. Yang, Y. Xia, W. Hu, J. Jing, and L. Chen, "Dynamic Island Partition Strategy for Active Distribution System with Controllable Load Participation," in 2020 IEEE Sustainable Power and Energy Conference (iSPEC), Nov. 2020, pp. 1927–1932.

[15] X. Gu and H. Zhong, "Optimisation of network reconfiguration based on a two-layer unit-restarting framework for power system restoration," IET Gener. Transm. Distrib., vol. 6, no. 7, p. 693, 2012.

[16] S. Li, L. Wang, X. Gu, H. Zhao, and Y. Sun, "Optimization of loop-network reconfiguration strategies to eliminate transmission line overloads in power system restoration process with wind power integration," International Journal of Electrical Power & Energy Systems, vol. 134, p. 107351, Jan. 2022.

[17] W. Liu, L. Sun, Z. Lin, F. Wen, and Y. Xue, "Multi-objective restoration optimisation of power systems with battery energy storage systems," IET Generation, Transmission & Distribution, vol. 10, no. 7, pp. 1749–1757, 2016.

[18] H. Sekhavatmanesh and R. Cherkaoui, "Analytical Approach for Active Distribution Network Restoration Including Optimal Voltage Regulation," IEEE Transactions on Power Systems, vol. 34, no. 3, pp. 1716–1728, May 2019.

[19] H. T. Nguyen, J. Muhs, and M. Parvania, "Preparatory Operation of Automated Distribution Systems for Resilience Enhancement of Critical Loads," IEEE Transactions on Power Delivery, vol. 36, no. 4, pp. 2354–2362, Aug. 2021.

[20] C. Contreras, A. Triviño, and J. A. Aguado, "Distributed Model Predictive Control for voltage coordination of large-scale wind power plants," International Journal of Electrical Power & Energy Systems, vol. 143, p. 108436, Dec. 2022.
[21] M. M. Adibi and D. P. Milanicz, "Estimating restoration duration," IEEE Transactions on Power Systems, vol. 14, no. 4, pp. 1493–1498, Nov. 1999.
[22] J. Zhou, "Optimization of the Fast Frequency Regulation Strategy for Energy Storage-Assisted Photovoltaic Power Stations," Distributed Generation & Alternative Energy Journal, pp. 263–296, Feb. 2024.
[23] N. Nazir and M. Almassalkhi, "Guaranteeing a Physically Realizable Battery Dispatch Without Charge-Discharge Complementarity Constraints," IEEE Trans. Smart Grid, vol. 14, no. 3, pp. 2473–2476, May 2023.

Biographies

Hongtao Li received the bachelor's degree in electrical engineering from Tianjin University in 1997 and the master's degree in electrical engineering from North China Electric Power University in 2005, respectively. He is currently working as a professor of engineering at State Grid Beijing Electric Power Company. His research areas include smart grid distribution system and New Electric Power System.

Tian Hao received his master's degree in electrical engineering from North China University of Technology. He is currently working as a teacher at Wuxi University. He is mainly engaged in energy Internet planning, power system reliability assessment, power system analysis, power grid planning and other research work.

Zijin Li received the bachelor's degree in renewable energy North China Electric Power University in 2011 and 2014. She is currently working as a senior engineer at State Grid Beijing Electric Power Company. Her research areas include hybrid ac/dc distribution network and microgrid.

Erang Zhao received the bachelor's degree in electrical engineering from Hebei of University Technology in 2014 and the master's degree in electrical engineering from Tsinghua University in 2021, respectively. He is currently working as a researcher at Department of Electrical Engineering, Tsinghua University. His research areas include power system operation and planning, microgrid operation.

Chen Wang was born in Beijing, China, in 1994. He received the B.S. and M.S. degree in electrical engineering from China Agricultural University, Beijing, China, in 2017 and 2021. His main research interests include hybrid ac/dc distribution network, renewable energy generation, and active distribution networks.

Lina Xu received the bachelor's degree in Electronic Information Science and Technology from Xuzhou University of Engineering in 2018. She is currently working at Wuxi Research Institute of Applied Technologies, Tsinghua University. She is mainly engaged in engineering software development work.